

STIS CCD Anneal Results

Michael A. Wolfe, James Davies, Charles Proffitt, Paul Goudfrooij, and
Rosa Diaz
April 15, 2009

ABSTRACT

In this ISR we give the results of the monitoring program for the STIS CCD average dark current and annealing accumulated during the lifetime of STIS (February 1997 to August 2004). This program consists of monitors of darks, biases, the growth of hot pixels, and the effect that annealing has on the elimination of these hot pixels. We find that the STIS CCD grew a number of hot persistent pixels (i.e., hot pixels which do not anneal away), and that it continued to grow hot pixels at a consistent rate before and after the switch from Side-1 electronics to Side-2 electronics. We also find that the STIS CCD annealed away new hot pixels at the ~81% rate when running under Side 1, and ~48% rate when running under Side 2.

Introduction

The STIS CCD is a SITe 1024×1024 back-illuminated thinned CCD. The pixels are 21 microns square, and the CCD is optimized to give a maximum quantum efficiency in the near-UV and visible. This particular CCD was chosen in order to allow first-order visible spectroscopy, target acquisitions, imaging, and partial backup for the near-UV MAMA. The initial readout noise was quite low (3.78 e^- ; Goudfrooij et al. 1997), and at the first anneal the raw mean dark current including all hot pixels was $\sim 0.0025 \text{ e}^-/\text{sec}$ at -83C . The quantum efficiency is quite good, greater than 60% at 5000 \AA decreasing to $\sim 20\%$ at 3000 \AA and 9000 \AA . The full range of spectral response for the CCD is from $\sim 2000 \text{ \AA}$ to 11000 \AA (Baum et al. 1996).

However, like all CCDs, the detector is subject to cosmetic defects, of which the most serious are charged particle hits (cosmic rays), hot pixels (pixels that retain and gain

charge), and bad rows and columns. Radiation damage inflicted on the CCD causes dark current and hot pixels to increase as a function of time. Annealing can remove some of the hot pixels, but on the whole, both the dark current and hot pixels will increase with time. The STIS CCD is monitored to track the variations on the dark and bias levels of the CCD at the two routinely used GAIN settings (1 and 4), to track the cosmic ray rate and hot pixel growth, and to verify the utility of the monthly anneals for the removal of hot pixels.

The Anneal Program

The STIS CCD is annealed every four weeks to minimize the number of hot pixels within the CCD. The anneal process itself is on the order of 16 hours long, which is sufficient time to allow the CCD to warm up from its operating temperature of -83 C to the ambient instrument temperature of roughly +5 C. To monitor the usefulness of the anneal, we regularly obtain pre- and post-anneal biases, darks and flats. We have analyzed the anneal program data from Cycles 7 through 12 (programs 7635, 8081, 8410, 8841, 8906, 9612 and 10022) in a uniform way. For each visit of each calibration program, a bias and a series of darks and flats were taken. It was found that 5 separate integrations (*i.e.*, a CR-SPLIT=5) were needed to allow for the best detection and elimination of cosmic rays in the individual darks. Biases and flats have a CR-SPLIT = 3. However, for the July, August and November 1997 anneals, a CR-SPLIT = 3 was used for the darks by mistake and the result of this mistake is seen in the figures as arrows representing either an upper (pointing down) or lower (pointing up) limit to these data points. These biases, darks and flats are obtained immediately before and immediately after the anneal takes place. Once the data are retrieved from the archive, the darks are recalibrated using the latest versions of calstis and co-added in order to form pre- and post-anneal darks. For the analysis reported in this ISR, we have used the contemporaneous biases to produce darks.

The overall purpose of the anneal program is to:

1. compare the pre- and post-anneal darks;
2. compare the numbers of hot pixels before and after the anneal to see if the numbers of hot pixels decrease;
3. determine whether the pre-anneal hot pixels actually anneal out or just become weaker.

In Table 1 we show an example of the observations occurring either before or after an anneal.

Table 1. Structure of STIS CCD Anneals

Target Name	Aperture	Optical Element	CR-SPLIT	Integration Time
Bias	50CCD	Mirror	3	0s
Dark	50CCD	Mirror	5	1200s
Imaging flat	50CCD	Mirror	3	0.6s
Spectral flat	52X2	G750M at $\lambda = 6768\text{\AA}$	3	0.1s

Analysis

In order to ensure a uniform and straightforward analysis of the efficiency of the anneals, Jeff Hayes wrote and delivered to the **xstis** package a STSDAS task called **anneal_darks**. This task is for the use of the STScI STIS team only. This script and wrappers for it have been modified over the years by Diaz and Davies to automate the production of flats and to allow for temperature scaling of the darks required by the switch to Side-2 electronics (discussed later in this ISR).

The task presumes that one has run **calstis** on the pre- and post-anneal darks and created a CRJ file. These CRJ files we call *corrected darks* for the sake of this paper. **anneal_darks** will, when given the pre- and post-anneal corrected darks, automatically generate a pair of re-normalized corrected darks (i.e., normalize the corrected darks to 1 sec), construct histograms of these re-normalized corrected darks, compute the mean, median, and standard deviation of the re-normalized corrected darks, and find the brightness, the number and the positions of the hot pixels present in both the pre- and post-anneal darks (i.e., which pixels do not anneal out). We have chosen to re-normalize the corrected darks by their total integration times to allow the analysis to be conducted directly in electron/sec/pixel. The task is written to facilitate the tracking of hot pixels that do not anneal out.

Discussion

The overall results of the analysis are presented in Figure 1. The number of post-anneal hot pixels at all count rate thresholds have increased linearly over time, but the slope of this trend changed between Side-1 and Side-2 operations (see discussion in the Predictions of Future Behavior section). It is important to distinguish between persistent hot pixels that last for a number of anneal cycles and new transient hot pixels that are healed by the anneal. We will discuss both of these classes in more depth later.

Effect of the Switch to Side-2 Electronics on STIS Anneals

STIS went into safe mode in May 2001 due to a blown fuse in the power line feeding the instrument, and there was a subsequent switch to redundant Side-2 electronics in July 2001. The Side-2 electronics do not have an active temperature control (the Side-2 thermistor used for temperature control of the CCD failed before launch and was not replaced), so there is no temperature regulation of the CCD. Thus the cooler runs all the time and keeps the CCD at a lower operating temperature than operations under Side-1, but this temperature fluctuates. We track this fluctuation by monitoring the CCD housing temperature, which is reported in the telemetry. The fluctuation in temperature causes the dark rate to fluctuate (see Tom Brown's ISR *STIS 2001-03*), and the two fluctuations are correlated. Not only does the dark rate depend upon the temperature of the CCD, but also the strength of that temperature dependence depends on the dark rate itself.

In order to keep the analysis of the annealing process as consistent as possible with previous anneals and the pipeline dark products, it is necessary to scale the darks to a reference CCD housing temperature, chosen as 18 C (Brown 2001). The CCD housing temperature is found in the header keyword OCCDHTAV in the first extension [1] of each STIS dark file. Both the housing temperature and the reference temperature are used to normalize the corrected darks. Each dark frame is scaled by a constant factor depending upon the temperature (*i.e.*, 7% per C), to place it at a level appropriate for the chosen reference temperature (*i.e.*, 18 C). The normalization used is given by the following expression:

$$(\text{corrected dark}) * (1 + 0.07(T_0 - T))$$

where corrected dark is the dark being normalized, T_0 is the reference temperature, and T is the CCD housing temperature. Note that the old (Side-1) set point was -83 C; however, since the move to Side-2 operations the mean T is now colder, and since the thermistor for Side-2 does not work there is no direct measure of T .

Because the CCD is operating at lower temperatures, there is an offset between the May and June 2001 anneal data as seen at day ~1600 in Figure 1, which shows the total number of post-anneal hot pixels dropping significantly. Since the dark rate depends on the temperature of the CCD and the strength of that dependence depends on the dark rate itself, the rate of increase in post-anneal hot pixels is lower than in operations under Side-1. Since we apply only a linear correction to scale the dark rate to a reference temperature, there is an increase in scatter in the post-Side-2 data, *i.e.*, we do not correct for any second order effects, and this shows up as scatter in the post-anneal dark rate over time and thus scatter in the post-anneal hot pixel number over time.

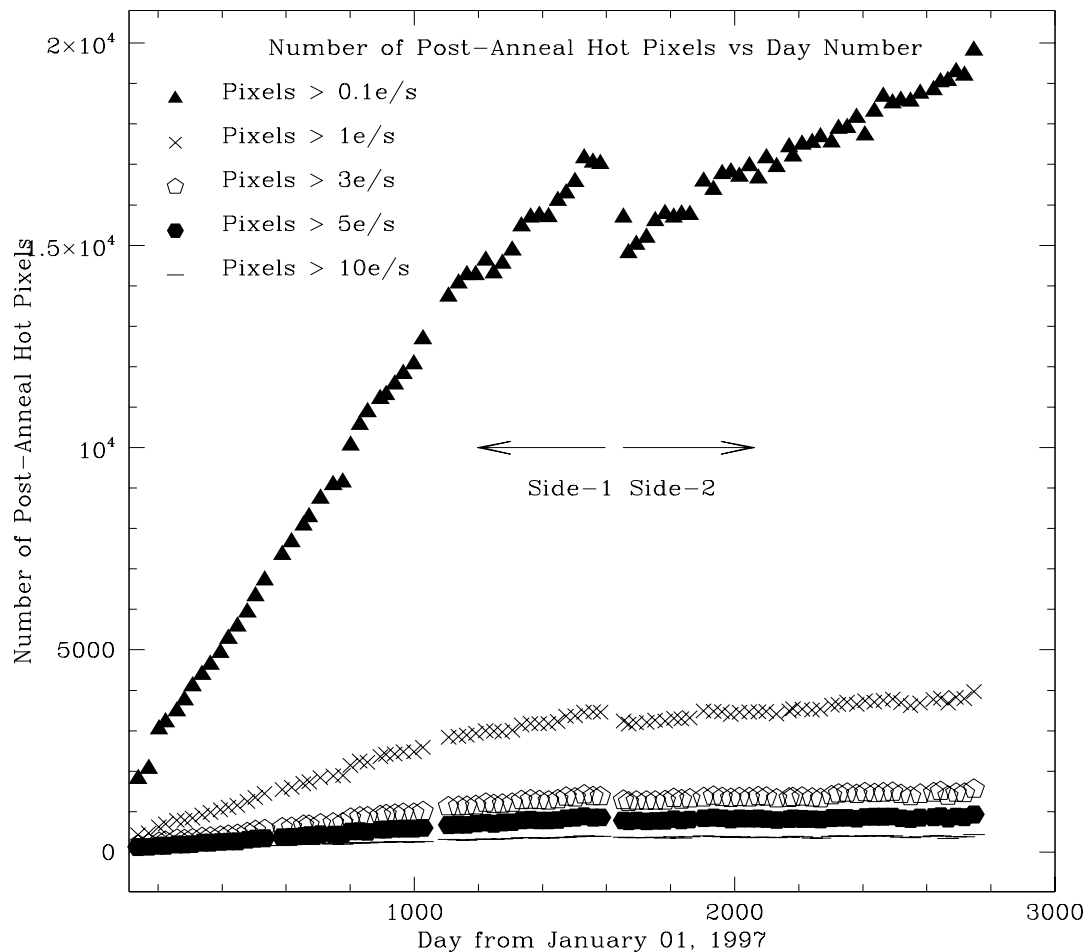


Figure 1: Number of post-anneal hot pixels vs. day number. The total number of permanent hot pixels increases linearly with time for the STIS CCD. The plot shows the total number of post-anneal hot pixels at different count-rate cuts. Notice that the rate of increase decreases due to the CCD running at cooler temperatures after the switch to Side 2, but that it remains linear. Also note that the scatter is greater due to the fluctuating temperatures after the switch to Side 2. The date that STIS switched to Side-2 is indicated by the arrows.

Side-1 and Side-2 STIS Anneals

In Figure 2, we plot the raw mean post-anneal dark count rate (*imstat* is set to 0 iteration for sigma clipping so no clipping is done resulting in a “raw” mean, which includes all hot pixels) as a function of time, with error bars of 1σ about the mean. The plot clearly shows a rising trend in the raw mean dark count rate well outside the 1σ error, implying that equilibrium has not been reached, and appears to be increasing with roughly linear behavior.

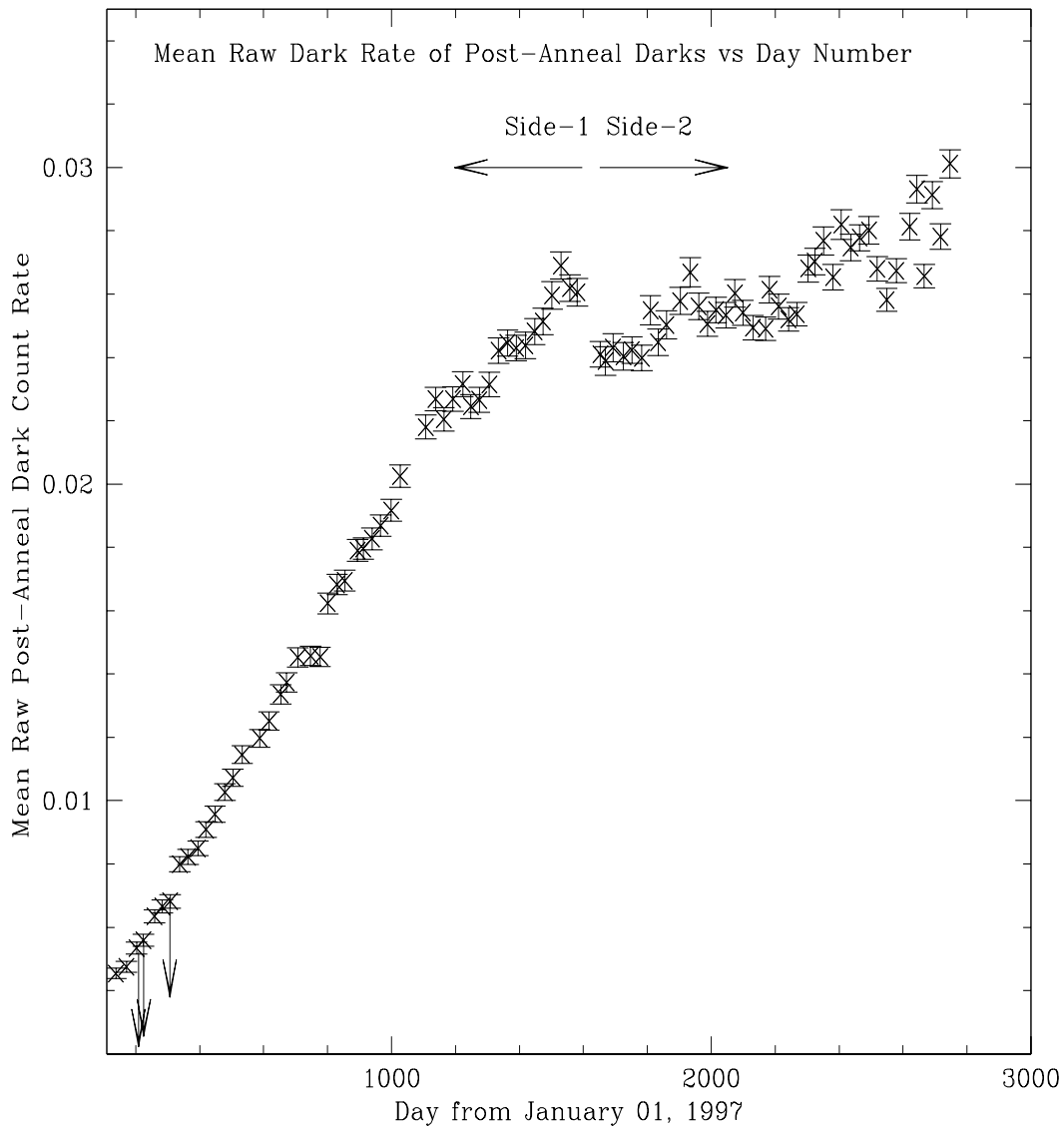


Figure 2: Mean raw dark rate of post-anneal vs day number. The plotted raw mean of each post-anneal corrected dark has error bars of $\pm 1\sigma$. The date that STIS switched to Side-2 is indicated by the arrows. The arrows represent an upper limit to some of the early data points because a CR-SPLIT = 3 was mistakenly used for these dark files.

In Figure 3, we plot the median post-anneal dark count rate (with 30 clipping cycle iterations and a 5σ clipping factor used by *imstat* resulting in median dark rate, which has had the hot pixels removed) as a function of time, with error bars of 1σ about the median. The plot clearly shows a rising trend in the median dark count rate well outside the 1σ error,

implying that equilibrium has not been reached, and appears to be increasing in a roughly linear trend.

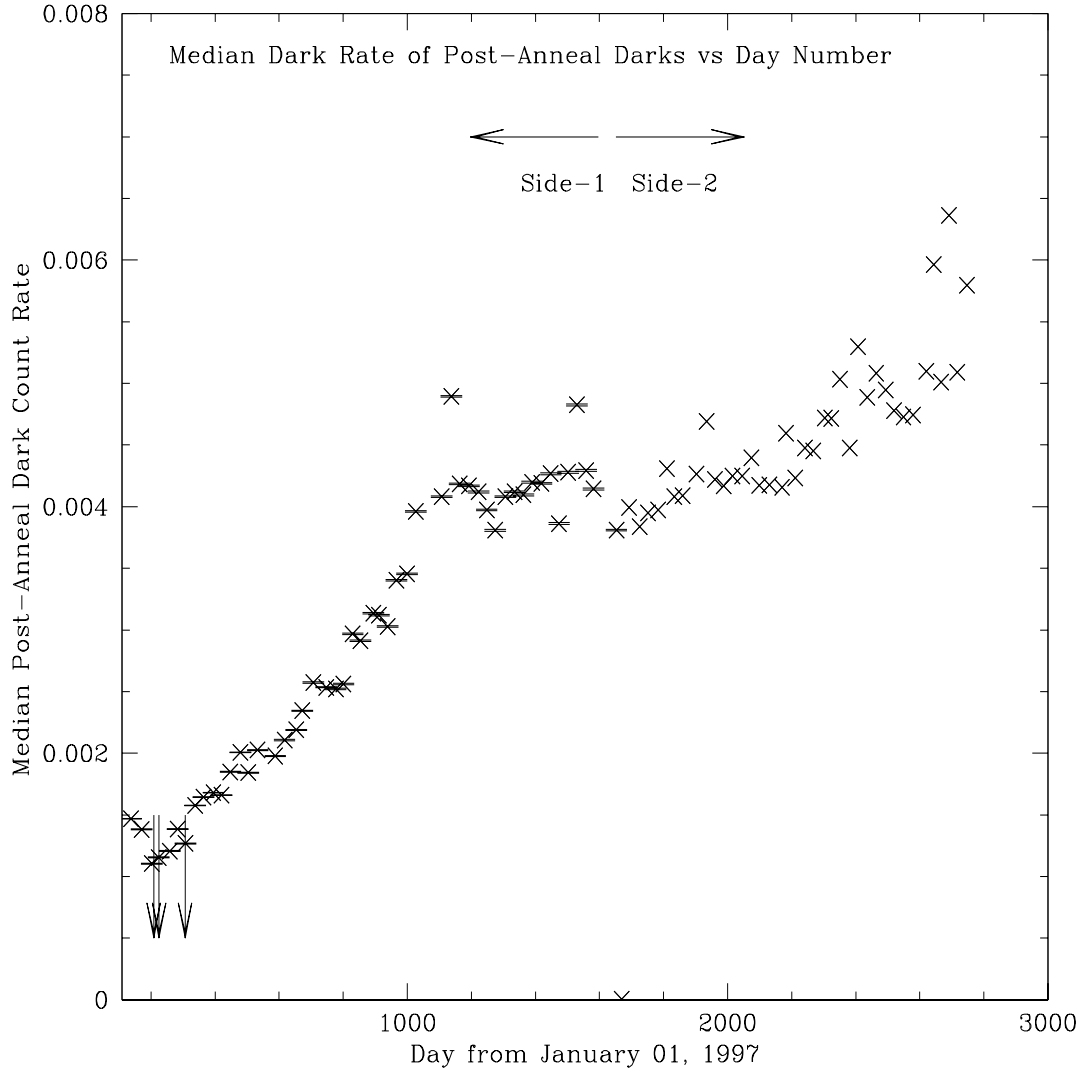


Figure 3: Median dark rate of post-anneal vs day number. Error bars of $\pm 1\sigma$ are given. Note that the errors for Side-2 are much smaller than the symbols denoting the data points. The date that STIS switched to Side-2 is indicated by the arrows. The arrows represent an upper limit to some of the early data points because a CR-SPLIT = 3 was mistakenly used for these dark files.

The rate of growth of hot pixels is defined as the number of hot pixels remaining after an anneal. The xstis package `anneal_darks` uses `imstat` to flag pixels that remain hot after iterating 30 times with 5σ clipping factor. In Figure 4, the rate of growth of pixels hotter

than $0.1e^-/\text{sec}$ are plotted as a function of day number. There are variations of up to 100 in the growth rate of these pixels. We also note that for pixels at higher cuts (1.0 and $10e^-/\text{sec}$), the variations in the rates of growth are much smaller, and show evidence of flattening out for Side-1. Side-2 electronics, however, show a creation rate that is more sporadic than for Side-1, due to a lack of temperature control. Therefore, it is difficult to determine if there will be any asymptotic behavior, if at all, for the creation rates. It does seem, however, that for Side-1 electronics the creation rate seems to be declining for the hot pixel level $0.1e^-/\text{sec}$, while for the hot pixel level $0.1e^-/\text{sec}$ for Side-2 this decline is not readily apparent. This lack of decline in the Side-2 creation rates is directly related to the lack of thermal control.

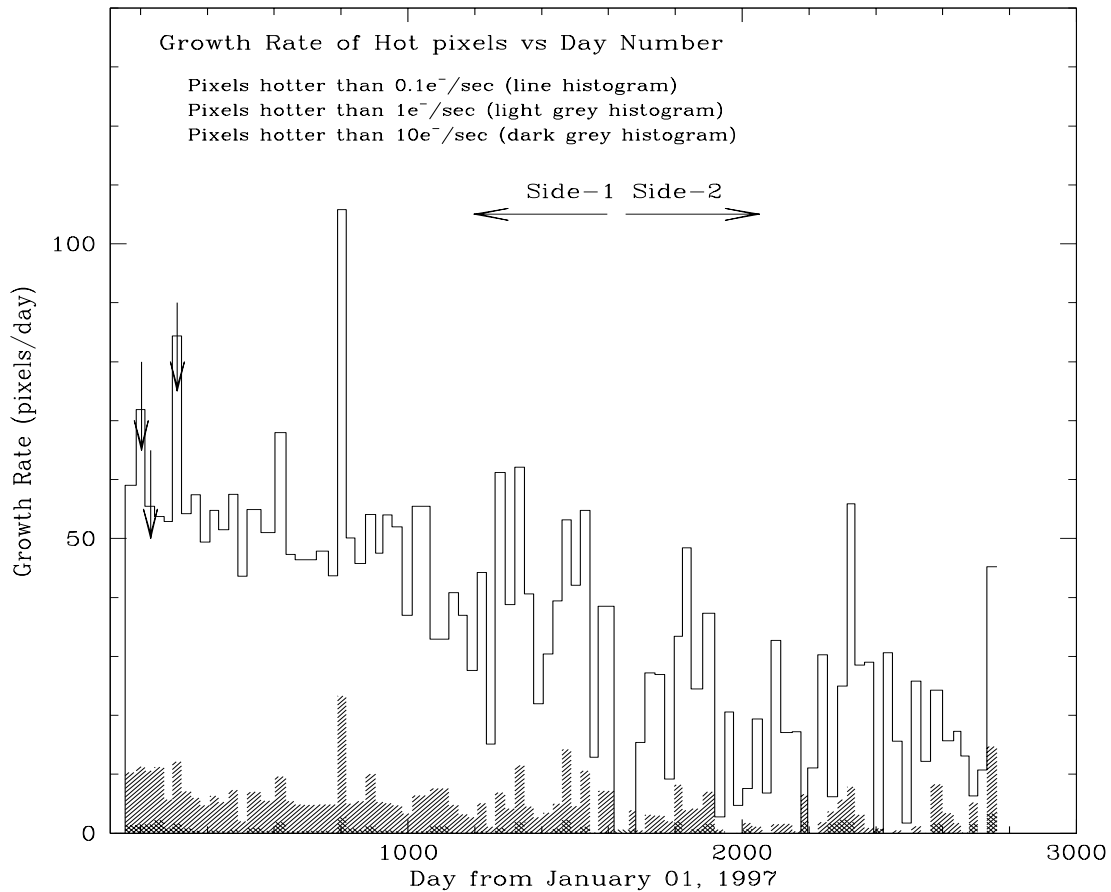


Figure 4: Histogram of the total growth rate of hot pixels vs. day number for the STIS CCD. The unshaded histogram is for pixels hotter than $0.1e^-/\text{sec}$; the light shaded histogram is for pixels hotter than $1.0e^-/\text{sec}$; and the dark shaded histogram is for pixels hotter than $10e^-/\text{sec}$. Side-1 and Side-2 in the figure represent the dates for which Side-1 and Side-2 electronics operate. The arrows represent an upper limit to some of the early data points because a CR-SPLIT = 3 was mistakenly used for these dark files.

Persistent pixels

In Figure 5 it is found that for the hot pixel level $1.0e^-/\text{sec}$, the percentage of hot pixels remaining after an anneal steadily increased from $\sim 85\%$ to $\sim 90\%$ for Side-1, while Side-2 remained at an average of $\sim 90\%$. It appears that the percentage of persistent number of pixels has stabilized. For the $0.1e^-/\text{sec}$ hot pixel level the percentage of persistent hot pixels, for both Side-1 and Side-2, is approximately 90% . In addition, while the percentage of persistent pixels decreases with the hot pixel level cut used (for pixels hotter than $10e^-/\text{sec}$ only about 75% of the pixels persist for Side-2), the trend is the same: the numbers of persisting hot pixels remains approximately the same from anneal to anneal, especially for Side-2. We have seen that, on average, $\sim 85\%$ of pixels that were hotter than $0.1e^-/\text{sec}$ before the anneal persist after that anneal. It would seem that our anneals are of only limited effectiveness in removing these very hot persistent pixels. If a more in depth discussion of Side-1 electronics is required, please see Hayes et al. (1998).

Transient pixels

In Figure 6, we plot the number of pre- and post-anneal hot pixels. Their difference is an upper limit to the number of transient pixels. This is because, in some cases, a percentage of persistent pixels (that are hot for several anneal periods) have been annealed. Another effect is that new pixels have become chronically hot. Therefore, the number of transient pixels is what remains after considering these two effects.

The STIS anneal program repairs transient hot pixels at a rate defined by

$$R_{CCD} = (\eta_{pre} - \eta_{post})/(\eta_{pre} - \eta_{post,prev}) \quad (1)$$

where:

η_{pre} = number of hot pixels pre-anneal for a given month

η_{post} = number of hot pixels post-anneal for a given month

$\eta_{post,prev}$ = number of hot pixels post-anneal for the previous month.

The above equation can be translated into “the number of hot pixels that annealed away in a given month divided by the number of new hot pixels that appeared in that month.”

In Figure 7, we plot the percentage of new pixels annealed, which is derived by multiplying equation 1 by 100. We see that the average annealing rate was about 81% for $0.1e^-/\text{sec}$ pixels during Side-1 operations. At times we seem to repair 100% our new hot pixels, but of course this is not the case as we can have new hot pixels persisting, while we have annealed away some older persistent pixels. After the switch to Side 2 on day ~ 1600 , there is a noticeable increase in the scatter of the rates, and the average rate for $0.1e^-/\text{sec}$ pixels drops below 48% . It seems that despite the fact that the CCD is run at cooler tem-

peratures the lack of thermal control decreases the effectiveness of the anneal process and introduces scatter in the percentage of hot pixels that are repaired.

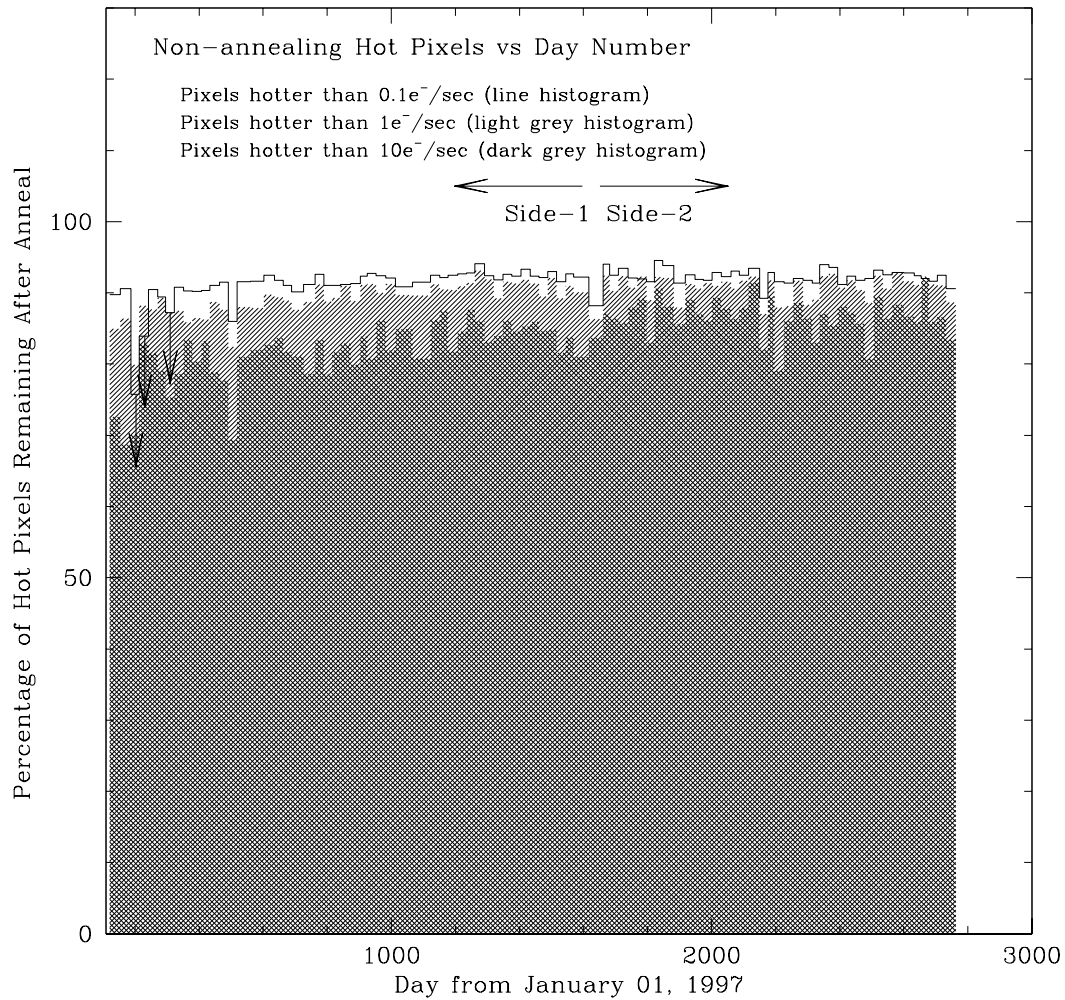


Figure 5: Histogram of the percentage of all hot pixels that persist after each anneal vs. the day number. We plot the percentage of pixels hotter than $0.1e^-/\text{sec}$ in the unshaded histogram, the percentage brighter than $1e^-/\text{sec}$ in the lightest shaded histogram, and the percentage brighter than $10e^-/\text{sec}$ in the darkest shaded histogram. Side-1 and Side-2 in the figure represent the dates for which Side-1 and Side-2 electronics operated. The arrows represent an upper limit to some of the early data points because a CR-SPLIT = 3 was mistakenly used for these dark files.

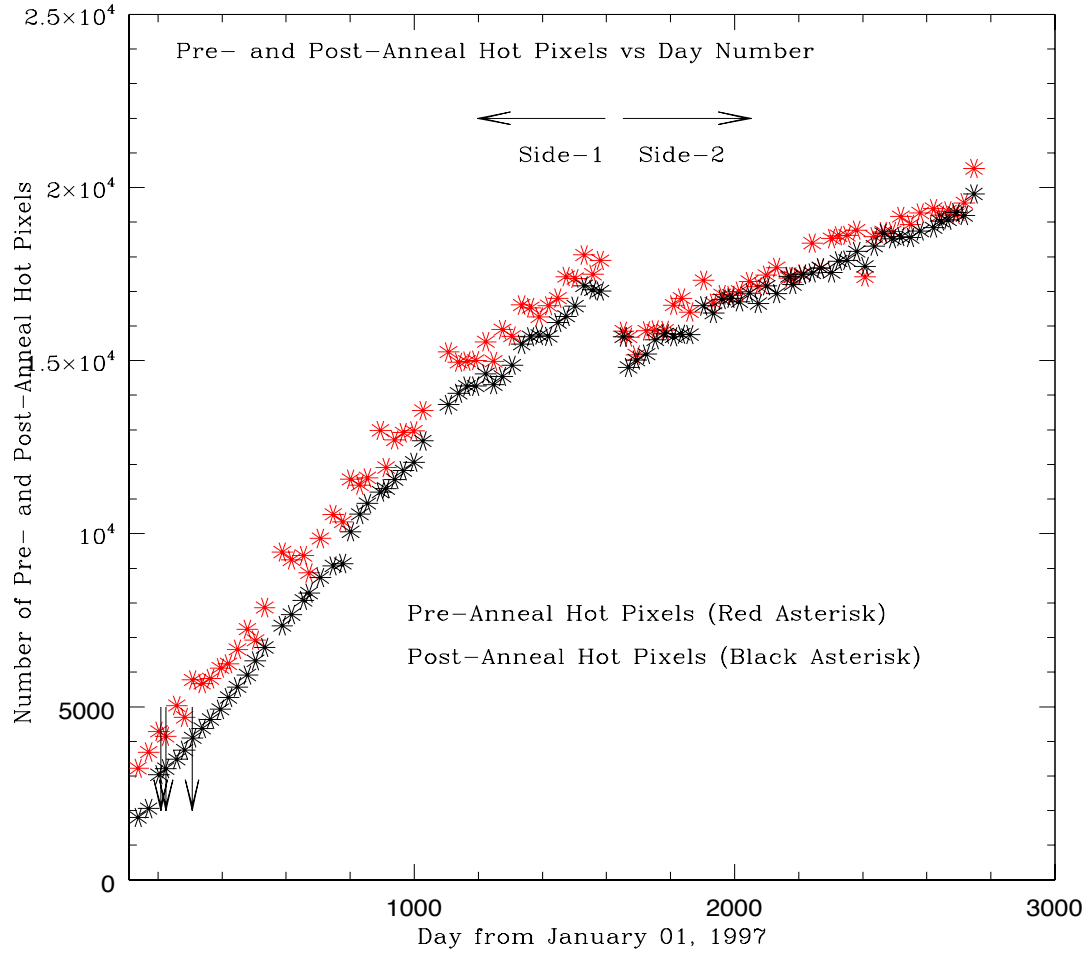


Figure 6: Plot of the number of pre and post-anneal hot pixels vs time. The only hot pixels level plotted here is $0.1e^-/\text{sec}$. The difference between the number of pre- and post-anneal hot pixels is a measure of the number of transient hot pixels. Side-1 and Side-2 in the figure represent the dates for which Side-1 and Side-2 electronics operated. The arrows represent an upper limit to some of the early data points because a $\text{CR-SPLIT} = 3$ was mistakenly used for these dark files.

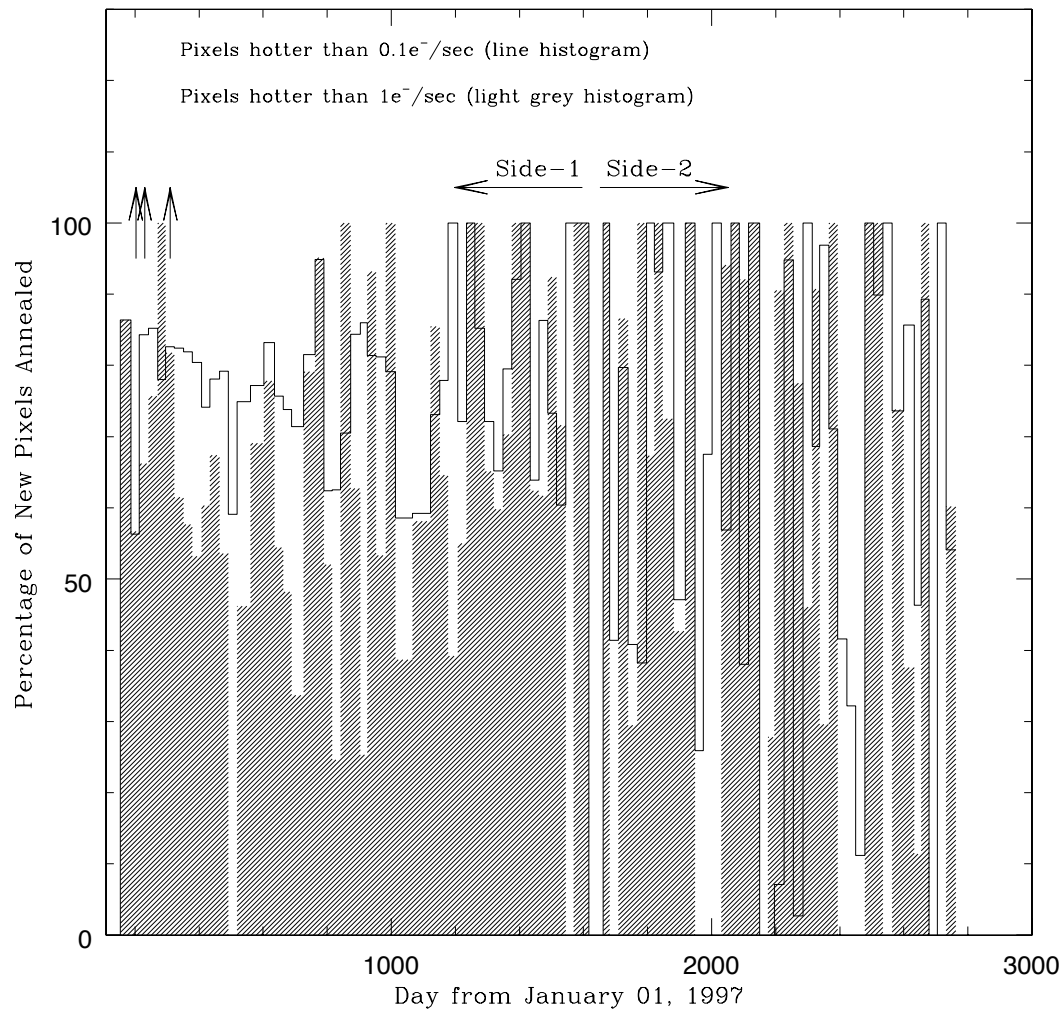


Figure 7: Percentage of new hot pixels annealed in a given month vs. the day number. The unshaded histogram is for all pixels brighter than 0.1e⁻/sec, while the shaded histogram is for pixels brighter than 1e⁻/sec. Side-1 and Side-2 in the figure represent the dates for which Side-1 and Side-2 electronics operated. The arrows represent a lower limit to some of the early data points because a CR-SPLIT = 3 was mistakenly used for these dark files.

Predictions of Future Behavior

To summarize our findings:

1. the STIS CCD continues to produce, at gross levels, large numbers of hot pixels (*i.e.*, pixels brighter than or equal to 0.1e⁻/sec);

2. for Side-2 the growth rate of these hot pixels has not reached equilibrium and is still increasing;
3. the percentage of hot pixels remaining after an anneal remains relatively constant over time;
4. every month we anneal 80% of new hot pixels;
5. for cuts brighter than $1e^-/\text{sec}$, the growth rate of new hot pixels is at a much slower rate.

If we again look at Figure 1, we note that the overall post-anneal hot pixel creation rate appears to be roughly linear. Assuming this to be the case, we have performed a linear least-squares fit to the post-anneal hot pixels to see if we can predict any trends. We find that the behavior of hot pixels with an electron level cut of $0.1e^-/\text{sec}$ data is well reproduced by a linear fit, where the results obtained for Side-1 and Side-2 are:

$$N_{cr} = 917.74 + 10.83\delta \quad \text{Side-1} \quad (2)$$

$$N_{cr} = 8719.90 + 3.92\delta \quad \text{Side-2} \quad (3)$$

where N_{cr} is the number of post-anneal hot pixels and δ is the number of days since January 01, 1997. The correlation coefficient for these data is 0.9956 for Side-1 and 0.9860 for Side-2 (an excellent linear fit). We have similar relations for the $1e^-/\text{sec}$ data and the $10e^-/\text{sec}$ data:

$$N_{cr} = 253.19 + 2.16\delta \quad \text{Side-1} \quad (4)$$

$$N_{cr} = 2243.60 + 0.588\delta \quad \text{Side-2} \quad (5)$$

for the $1e^-/\text{sec}$ data, having a correlation coefficient of 0.9937 for Side-1 and 0.9578 for Side-2; and

$$N_{cr} = 26.67 + 0.236\delta \quad \text{Side-1} \quad (6)$$

$$N_{cr} = 321.71 + 0.025\delta \quad \text{Side-2} \quad (7)$$

for the $10e^-/\text{sec}$ data, having a correlation coefficient of 0.9957 for Side-1 and 0.4302 for Side-2, which is not as good as for lower electron level cuts.

Note that for all three of the Side-1 fits we have omitted the data from day 109 because the CCD was still being cooled down to its working temperature at this time. If we use the linear regression for the $0.1e^-/\text{sec}$ (using the Side-2 linear fit, equation 3), we find that about 2.6% of all our pixels will be persistently hot on October 31, 2010 (end of Cycle 17). Using the Side-2 linear fit, we find that we will need ~ 67 years to reach the 10% mark. This, of course, assumes that the rate of increase remains constant. For hotter pixels, the time to reach the 10% mark would be substantially longer. As can be seen from Table 4, our tabulation of the predictive models, the agreement between the already observed and the predicted count rates is very good.

Table 2. Predictions of STIS CCD post-anneal hot pixel growth for Side-2.

Day Number from 1-Jan-1997	Predicted Number of Pixels 0.1 e/sec	Measured Number of Pixels 0.1 e/sec	Predicted Number of Pixels 1 e/sec	Measured Number of Pixels 1 e/sec	Predicted Number of Pixels 10 e/sec	Measured Number of Pixels 10 e/sec
1653	15199	15683	3215	3236	363	367
1934	16301	16396	3380	3354	370	393
2242	17508	17532	3561	3511	377	351
2464	18378	18677	3692	5268	383	398
2643	19080	19032	3797	3804	387	403
2747	19488	19816	3858	3972	390	428

In Figure 3, the median dark count rate for Side-2 appears to be roughly linear. Assuming this to be the case, we perform a linear least-squares fit and derive the following equation:

$$D_{rate} = 0.003756 + 1.507 \times 10^{-6} \beta \quad (8)$$

where β is the day number from July 10, 2001 and D_{rate} is the median dark count rate. The correlation coefficient is 0.8455 and this poor fit illustrates the lack of thermal control for Side-2 operations. Adopting this relation, we find that the median dark count rate for October 31, 2010 is 0.008878 cts/pixel. The count rate for August 03, 2004 (the day STIS ceased operations) is 0.005444 cts/pixel. The median dark count rate will have increased by ~39% over this time span. It should be noted, however, that it is difficult to anticipate what the median dark count rate will be after STIS is repaired so it is uncertain whether equation 8 will accurately predict the median dark count rate. On the other hand, the three-month safing period prior to SMOV3a failed to appreciably affect any long term trends. Only data gathered during the SMOV for SM4 (assuming STIS is fixed) will determine whether the dark count rate is appreciably different than the values derived from equation 8.

At the present time, about 2.6% of the STIS pixels are persistently hot. Once STIS is operating again, we will resume the anneal program and monitor the rate of growth and persistence of hot pixels.

Acknowledgments

We would like to thank Jeff Hayes and Jennifer Christensen for their significant contribution leading to the first Anneals ISR, on which this ISR is based.

References

- Baum., S.A. et al.; 1996 *STIS Instrument Handbook* Version 1.0 (Baltimore:STScI)
- Brown, T.M.; 2001 *Temperature Dependence of the STIS CCD Dark Rate During Side-2 Operations* STIS ISR 2001-03 (Baltimore:STScI)
- Feinberg, L. et al.; 2000 *STIS CCD Read Noise Anomaly Review Board Final Report* (Greenbelt:GSFC)
- Goudfrooij, P., Beck, T., Kimble, R., Christensen, J.A.; 1997 *STIS Results from SMOV: CCD Baseline Performance* STIS ISR97-10 (Baltimore:STScI)
- Hayes, J.J.E., Christensen, J.A., Goudfrooij, P.; 1998 *STIS CCD Anneals* STIS ISR98-06-Revision A (Baltimore:STScI)